Research Article

*International Journal of Advanced Technology and Engineering Exploration, Vol 12(126)*
*ISSN (Print): 2394-5443 ISSN (Online): 2394-7454*
*http://dx.doi.org/10.19101/IJATEE.2024.111100597*

# A deep learning framework for ECG Arrhythmia classification using GAM-ResNet18 and Namib beetle optimization-based domain adaptation

**Lakshmi Naga Jayaprada Gavarraju[1], Sandhya K[2], Tejesh Reddy Singasani[3], Dileep Pulugu[4], Lokesh Sai Kiran Vatsavai[5], Usha Rani Bajjuri[6], Ramesh Vatambeti[7*]**
Department of Computer Science and Engineering, Malla Reddy College of Engineering and Technology, Hyderabad 500100, Telangana, India[1]
School of Computing, Mohan Babu University, Tirupati 517102, Andhra Pradesh, India[2]
School of Computer and Information Sciences, University of the Cumberlands, Louisville, KY 40769, USA[3]
Department of Computer Science and Engineering, Malla Reddy College of Engineering and Technology, Hyderabad 500100, Telangana, India[4]
Department of Information Technology, SRKR Engineering College, Bhimavaram 534204, Andhra Pradesh, India[5]
Department of computer science and engineering, Lakireddy Bali Reddy College of engineering, Mylavaram 521230, Andhra Pradesh, India[6]
School of Computer Science and Engineering, VIT-AP University, Vijayawada 522237, Andhra Pradesh, India[7]

Received: 21-April-2024; Revised: 13-May-2025; Accepted: 16-May-2025


## Abstract
***The diagnosis of cardiac disorders using electrocardiograms (ECGs) is critical, yet it remains susceptible to variability and often requires time-consuming manual interpretation by experts. To enhance efficiency and reduce dependency on expert analysis, the development of automated and accurate diagnostic tools is essential. This paper proposes an innovative domain adaptation network (DAN), inspired by the Wasserstein distance and generative adversarial networks (GANs). The network utilizes labeled data from multiple subjects (source domain) to improve classification performance for ECGs in a target domain. Feature extraction is conducted using a global attention module-ResNet18 (GAM-ResNet18) deep learning (DL) model with transfer learning, focusing on critical features such as the R axis, T axis, and QRS count. The proposed architecture consists of a classifier, domain discriminator, and feature extractor, and incorporates attention mechanisms along with a variance layer to enhance signal-to-feature discrimination. The model was trained and validated on both original and noise-attenuated ECG signals from the Chapman dataset. Evaluation metrics including accuracy, precision, recall, and F1-score demonstrate the superior performance of the proposed model, particularly in arrhythmia detection—a task often hindered by noise and irregular events. This model presents a promising solution for automated and efficient arrhythmia diagnosis, addressing the limitations of traditional ECG analysis. Its integration of advanced techniques such as the Wasserstein distance, GANs, attention mechanisms, and transfer learning highlights its potential to significantly improve the diagnosis of cardiac disorders in clinical settings.***

## Keywords
***Electrocardiogram, Arrhythmia classification, Domain adaptation network, Generative adversarial network, Global attention module, Transfer learning.***

## 1.Introduction
Cardiovascular diseases (CVDs) are the leading cause of global mortality, accounting for nearly one-third of all annual deaths [1, 2]. In regions such as Russia, Asia, and the Middle East, CVDs pose a particularly significant health burden because of their high incidence rates [3].

Among various cardiac disorders, arrhythmias are a critical concern, primarily due to their association with abnormalities in the heart's electrical system [4].

Electrocardiograms (ECGs) are the standard diagnostic tool for detecting these arrhythmias. Globally, over 300 million ECGs are recorded annually [5, 6]. The non-invasive nature and cost-effectiveness of ECGs establish them as a preferred diagnostic method compared to more complex

*Author for correspondence

imaging techniques like computed tomography (CT) and magnetic resonance imaging (MRI) [7, 8].

Despite the widespread use of ECGs, manual interpretation presents several challenges. The varied morphologies of cardiac arrhythmias hinder accurate diagnosis, and dependence on visual identification introduces subjective biases, potentially compromising diagnostic accuracy [9–11]. As a result, the need for expert interpretation makes the process time-consuming and inconsistent [12, 13]. Deep learning (DL) techniques, such as recurrent neural networks (RNNs) and convolutional neural networks (CNNs), have demonstrated potential in automating arrhythmia detection. However, their opacity and limited interpretability have hindered widespread clinical adoption [13–15]. In healthcare, ensuring the transparency and accountability of DL models is critical, where decisions directly impact patient outcomes [16, 17].

This work is motivated by the need to overcome the limitations of existing ECG analysis methods. The current approaches are either too dependent on manual interpretation or fail to provide sufficient transparency for clinical decision-making. This study aims to develop a DL- based approach that not only improves diagnostic accuracy but also enhances interpretability, making it more suitable for clinical settings.

The primary objectives of this study are to design a domain adaptation network (DAN) leveraging the Wasserstein distance and generative adversarial networks (GANs) for robust ECG analysis. It aims to enhance feature extraction using the global attention module-ResNet18 (GAM-ResNet18) model integrated with attention mechanisms and variance layers. The overarching goal is to improve the accuracy and interpretability of cardiac arrhythmia detection in diverse, noise-prone datasets.

This paper introduces a novel domain adaptation framework combining Wasserstein distance-based alignment with GANs to address variability in ECG data across patient populations. The proposed GAM-ResNet18 model, enhanced with attention mechanisms and variance layers, extracts both spatial and temporal features for improved classification accuracy. Additionally, the study employs the Namib beetle optimization algorithm (NBOA) for efficient training, ensuring robustness against data imbalance and noise. The results demonstrate significant advancements over existing methods, particularly in detecting underrepresented arrhythmias, thereby contributing to the development of clinically reliable and interpretable diagnostic tools.

The remainder of the paper is organized as follows. Section 2 reviews relevant literature to provide context for the proposed approach. Section 3 outlines the methodology in detail. Section 4 presents the results of the experimental analysis and evaluates the performance of the proposed model. Section 5 discusses the findings, and section 6 concludes the paper with suggestions for future research.

## 2.Literature review

Integrating DL into ECG analysis has significantly advanced automated cardiac arrhythmia detection. However, the complexity of arrhythmia morphologies, class imbalances, and the need for interpretable models continue to present challenges. This section synthesizes key studies, linking their methodologies and findings to highlight thematic progress and gaps in the field.

Kim et al. (2024) proposed an automated network for arrhythmia classification using CNNs on 12-lead ECG data, achieving high accuracy across 45 arrhythmia types. However, the model's complexity limited its real-time applicability [18]. Similarly, Anand et al. (2024) compared CNN and ResNet-18 architectures, with ResNet-18 demonstrating slightly better accuracy. Nonetheless, its significant computational resource demands made it less feasible for resource-constrained environments [19].

Attention mechanisms, which enhance the focus on critical signal features, have emerged as a pivotal theme in improving arrhythmia detection. Darmawahyuni et al. (2024) incorporated fused features of the RR interval and QRS complex with attention-based DL, achieving high classification accuracy but encountering challenges with model interpretability [20]. Building on similar concepts, Kaniraja and Mishra (2024) developed a DL framework for ECG super-resolution, enhancing the classification of low-quality signals but introducing computational inefficiencies [21]. Additionally, Soman and Sarath (2024) used the Chameleon-Sparrow search algorithm (CSSA) to optimize deep convolutional neural networks (DCNNs), demonstrating superior accuracy and sensitivity but grappling with algorithmic complexity [22].

Recent advancements have also explored transformer-based architectures for arrhythmia detection. El-ghaish and Eldele (2024) proposed the ECGTransForm framework using bidirectional transformers, which effectively handled class imbalances and showed superior performance. However, interpretability issues remained a barrier to clinical adoption [23]. Similarly, Pasha et al. (2023) emphasized the need for interpretable models in ECG analysis, advocating for balancing model complexity and clinical transparency [24].

Optimization techniques and hybrid models have further enriched the field. Mahajan and Kaul (2024) employed a multi-stage filtering approach combined with shallow models, improving performance in simple arrhythmias but struggling with complex ones [25]. Gupta et al. (2022) demonstrated high accuracy using hybrid DL models but noted limitations due to the extensive data requirements for training [26]. In contrast, Hannun et al. (2022) achieved cardiologist-level performance using deep neural networks, though their black-box nature hindered interpretability [27]. Another emerging focus is improving model generalizability across diverse datasets. Zhang et al. (2021) explored interpretability techniques to enhance model transparency, addressing a critical requirement for clinical acceptance. However, this approach often came at the cost of reduced model complexity [28]. Ullah et al. (2023) proposed a 2-dimensional (2D) ECG spectral image representation approach for arrhythmia classification using DL. The method showed improved accuracy over traditional ECG analysis techniques, but the transformation of ECG signals into images added computational overhead [29].

Jin et al. (2024) explored interpretability techniques for DL models in cardiac arrhythmia diagnosis. They proposed a framework to enhance the transparency of DL models, but the added interpretability came at the cost of reduced model complexity [30]. Narotamo et al. (2024) surveyed DL approaches for ECG signal processing and classification, highlighting the need for models that balance accuracy with interpretability and computational efficiency [31]. Sraitih et al. (2022) developed an automated ECG arrhythmia detection system using machine learning techniques. The system showed promising results but was limited by its dependency on feature engineering, which can be time-consuming and data-specific [32]. While advancements in attention mechanisms, transformer-based approaches, and optimization algorithms have significantly improved arrhythmia detection, challenges in interpretability, computational efficiency, and generalizability persist. This work builds on these findings by leveraging a GAM-ResNet18 model enhanced with attention mechanisms and domain adaptation strategies, aiming to bridge the gap between performance and clinical applicability. Time is of the essence, expert interpretations might vary, and mistakes caused by signal noise and unpredictability are possible in the conventional method of analyzing ECGs for the diagnosis of cardiac disorders. The urgent need for a novel automated diagnostic tool to improve the reliability, precision, and timeliness of ECG analysis is addressed in this research. Our solution utilizes state-of-the-art machine learning approaches, such as a DL model and an upgraded DAN, to transform ECG diagnoses, drastically improving patient outcomes by reducing the occurrence of misdiagnosis.

## 3.Materials and methods

This study proposes a novel approach to cardiac arrhythmia diagnosis using advanced DL techniques combined with interpretability methods. The methodology is structured as follows:

**Data collection and preprocessing**

The study utilizes a comprehensive ECG dataset from the Chapman database, which includes recordings from over 10,000 individuals. The data is pre-processed to remove noise and artifacts, ensuring high-quality inputs for the model. The Chapman database was chosen for its comprehensive nature, providing high-quality labelled ECG data, which is essential for training robust DL models. Preprocessing ensures the removal of noise and artifacts that could negatively impact the model's accuracy.

**Feature extraction using GAM-ResNet18**

A ResNet-based model, GAM-ResNet18, is employed for feature extraction from ECG signals. The model is enhanced with a GAM module to improve feature selection. This stage also involves converting ECG signals into a suitable format for DL processing. ResNet18 was selected for its proven effectiveness in handling complex feature extraction tasks in DL. The addition of the GAM module enhances the model's ability to discriminate between critical features, a necessity when dealing with the intricate variations in ECG signals. Other models like the visual geometry group (VGG) or DenseNet were considered, but ResNet18 was preferred due to its balance between performance and computational efficiency.

**Domain adaptation network (DAN) design**

To address the variability in ECG data across different patients, a DAN is developed. This network leverages the Wasserstein distance matrix and GANs to align the source and target domains, thereby improving classification accuracy on new, unseen data. The Wasserstein distance was chosen over other domain adaptation methods like maximum mean discrepancy (MMD) because it provides a more effective and continuous measure of distribution divergence, particularly in DL tasks. GANs were incorporated to generate synthetic data that bridges the gap between the source and target domains, improving the model's adaptability.

**Incorporation of attention mechanisms and variance layer**

To enhance the model's interpretability and performance, the convolutional block attention model (CBAM) and a variance layer are integrated. These components are designed to focus on the most relevant features of the ECG signals, improving the model's ability to discriminate between different types of arrhythmias. CBAM was selected due to its ability to efficiently handle both channel and spatial attention, making it superior to traditional attention mechanisms that only focus on one aspect. The variance layer was incorporated to better capture time-related features of ECG signals, a critical factor in diagnosing arrhythmias, where timing irregularities are key. The model is trained using the NBOA, which dynamically adjusts the learning rate to optimize performance.

**Algorithm: Proposed GAM-ResNet18 with domain adaptation for arrhythmia detection**

**Input:** Pre-processed ECG signals from Chapman dataset

**Output:** Predicted arrhythmia class

**Initialize**: Load the ECG dataset.

Perform preprocessing: noise filtering, normalization, segmentation, and transformation to spectrogram format.

**Feature Extraction**:

Input ECG spectrograms into the GAM-ResNet18 network.

Extract spatial features using residual blocks enhanced with CBAM.

Compute temporal features using a variance layer.

**Domain adaptation**:

Align source and target domains using Wasserstein distance-based GAN.

Train feature extractor and domain discriminator adversarially.

**Classification**:

Train the classifier using labeled data from the source domain.

Predict the labels of target domain ECG signals.

**Optimization**:

Use Namib beetle optimization algorithm (NBOA) to optimize model parameters dynamically.

**Output**:

Evaluate the model using metrics such as accuracy, precision, recall, and F1 score.

## 3.1Data preprocessing

The ECG data, obtained from the Chapman database, underwent several preprocessing steps to ensure the quality and consistency of the input signals before being fed into the DL models. These steps are essential to reduce noise, remove artifacts, and ensure that the data is standardized for training the models. The preprocessing techniques employed include the following:

**Noise removal and filtering:**

ECG signals are often contaminated by noise, including power line interference, baseline wandering, and muscle artifacts. To address this, a Butterworth bandpass filter with a frequency range of 0.5 Hz to 40 Hz was applied. This range was selected to preserve the essential features of the ECG signal while filtering out high-frequency noise and low-frequency baseline drift.

**Normalization:**

The ECG signals were normalized to ensure that the data is on the same scale, which is critical for the proper functioning of DL models. Each ECG signal was min-max normalized to a range of [0, 1], which helps to avoid issues related to large-scale differences in input values and ensures that the network can learn effectively.

**Handling missing data:**

Any missing data points in the ECG signals were handled through linear interpolation. This technique was applied to estimate missing values by interpolating between neighbouring data points, ensuring continuity in the signal without introducing bias.

**Segmentation and resampling:**

To ensure consistency in input length, all ECG signals were segmented into 10-second windows. Since the sampling rate of the Chapman dataset is 500 Hz, this resulted in windows containing 5000 data points per segment. In cases where signals had varying lengths, we used resampling techniques to ensure all inputs to the model had a uniform size.

**Transformation into 2D image format:**
For the purpose of training the GAM-ResNet18 model, the 1-dimensional (1D) ECG signals were transformed into a 2D image format using a time-frequency representation. This transformation was achieved through the short-time Fourier transform (STFT), which converts the ECG signal into a spectrogram, providing a visual representation of the signal's frequency content over time.

## 3.2Arrhythmia dataset

Zheng et al.'s dataset, which includes ECG data from 10,588 individuals, was utilized in this investigation [33]. This dataset was derived from the Chapman database, which is maintained by Chapman University and Ningbo People's Hospital in Shaoxing. The dataset contains raw ECG signals from twelve leads and includes eleven clinically derived features, such as the QT interval, corrected QT (QTc), R axis, Q offset, and T offset [34, 35]. The 12-lead ECG dataset is comprised of 500 Hz-sampled signals that have been classified into eleven different rhythm classes. These include atrial flutter (AF), atrial fibrillation (AFIB), atrial tachycardia (AT), atrioventricular nodal reentrant tachycardia (AVNRT), atrioventricular reentrant tachycardia (AVRT), sinus irregularity (SI), sinus bradycardia (SB), sinus rhythm (SR), sinus intermittent rhythm (SINT), supraventricular arrhythmia with aberrant waveform rhythm (SAAWR) and supraventricular tachycardia (SVT). Murat et al. [36] consolidated patients from underrepresented classes into comparable categories to establish four distinct class labels using this dataset. *Table 1* displays the combined information for these four rhythm classes.

**Table 1** Merged ECG rhythm class labels

| Merged rhythms | New class |
|---|---|
| SR + SI | SR |
| AF + AFIB | AFIB |
| SB | SB |
| SVT + AT + SAAWR + SINT + AVNRT + AVRT | Generalized supraventricular tachycardia (GSVT) |

The abbreviations "AF," "AFIB," "AT," "AVNRT," and "AVRT" stand for atrioventricular re-entrant tachycardia and AF, respectively. SI: abnormalities of the sinuses the abbreviations SAAWR, SB, SR, SINT, and SVT respectively.

### 3.2.1Hyperparameter tuning

To optimize the model's performance, random search was applied for hyperparameter tuning, followed by grid search on the most promising hyperparameter combinations. The following hyperparameters were tuned:
Learning rate: Tested values: [0.001, 0.0001, 0.00001].
Batch size: Tested values: [16, 32, 64].
Dropout rate: Tested values: [0.2, 0.3, 0.4].
L2 regularization: Tested values: [0.0001, 0.0005, 0.001].

Random search allowed for a broad exploration of the hyperparameter space, while grid search focused on fine-tuning the most impactful parameters based on initial results.
Random search was selected initially to explore a wide range of hyperparameters efficiently, and grid search was employed for fine-tuning based on the most promising hyperparameter combinations. This dual-stage tuning method ensured that the model was not constrained by local optima and that the most effective hyperparameter values were selected.

## 3.3Design of GAM-ResNet18 network model for feature extraction

When it comes to picture categorization, ResNet18 is the DL model that most people use. The picture characteristics are extracted by means of convolution and pooling layers, while problems with model deterioration are addressed by means of residual blocks and fully connected layers. This research suggests the GAM-ResNet18 model, an upgrade on ResNet18 trained on ECG signal classification tasks. To improve feature selection for each residual block output, the GAM-ResNet18 model incorporates a GAM module. The module employs a multilayer perceptron to determine the weights linked to each channel and does global average pooling. To obtain a better output with more informative features, the original feature map is combined with the weighted feature map. The GAM-ResNet18 model outperforms ResNet18 in terms of feature selection capabilities after including GAM modules. Modelling begins with converting ECG data to an image format using residual blocks and GAM modules; next, time series features signals using the 2D convolution and max pooling layers. The characteristics include the following: R Wave Voltage (RV), T Axis (TA), QRS Count, Q Onset, AR, ventricular, and axial rates; QT interval, corrected and duration, R and T axes.

### 3.3.1GAM-ResNet18 network training

An 80:20 ratio divides the dataset into training set and a test set, with 20% of the training set kept aside for validation purposes. A batch size of 32 and a learning rate of 0.0001 are used for training the model with an image dimension of 224 × 224. To optimize the network, the NBOA is applied, which uses adaptive learning rates to dynamically adjust the update step size for each parameter. By speeding up the training process, this method avoids the problem of local optimization. Keeping an eye on the model's accuracy and loss value on the validation set allows us to evaluate its performance.

In contrast to accuracy, which is defined as the ratio of properly predicted samples to total samples, loss may be seen as the difference between the real labels. After the sixth epoch, the loss value on the validation set stabilizes. After the ninth epoch, the accuracy approaches the value from the training set. The results show that the model may be used in a wide range of situations.

### 3.3.2Fine-tuning of the model using NBOA

The Namib beetle typically makes its way downwards after drinking and gathering water, although lizards may catch a few of them in the act. On their journey return to the nest, they need to go via low-risk areas. Several research and practical efforts have utilized the behavior of these beetles to address the issue of water scarcity in the desert. In the desert, devices that capture air humidity have been made using the Namib beetle collecting approach. This article explains how the NBO algorithm finds the best solution by considering water seeking behavior, identifying a suitable mound for water collecting, and the chance of pursuing each beetle in identifying moisture. Each possible solution to the problem is represented by a beetle in the suggested approach and may be stored in the D dimensions, as shown in Equation 1.

$$NB = [x_1, x_2, x_3, \dots, x_D] \quad (1)$$

A decision variable D is present in every beetle. As shown in Equation 2, a portion of them can be fashioned at random as N values between L and U to serve as the starting population.

$$Pop = \begin{bmatrix} NB_{1,1} & NB_{1,1} & \cdots & \cdots & NB_{1,D} \\ NB_{2,1} & NB_{1,1} & \cdots & \cdots & NB_{2,D} \\ \vdots & \vdots & \iddots & \iddots & \vdots \\ \vdots & \vdots & \iddots & \iddots & \vdots \\ NB_{N,1} & NB_{1,1} & \cdots & \cdots & NB_{N,D} \end{bmatrix} \quad (2)$$

The starting population of beetles is represented by Pop in this equation. However, the beetle-related component is also shown by NB. Using Equation 3, one may generate any solution in the problem space at random.

$$NB_{i,j} = L + (U - L).rand(0,1) \quad (3)$$

Using the goal function, any problem solver or insect may be assessed in this case. In this case, we have function that shows the hill's height as the objective function. For optimization problems of the minimization kind, this objective function can be utilized. One way to assess the beetle population is to use the objective function, as shown in Equation 4.

$$Fitness = \begin{bmatrix} f(NB_{1,1,} & NB_{1,2} & \cdots & NB_{1,2}) \\ f(NB_{2,1} & NB_{1,2} & \cdots & NB_{1,2}) \\ \vdots & \vdots & \vdots & \vdots \\ f(NB_{N,1} & NB_{1,2} & \cdots & NB_{1,2}) \end{bmatrix} = \begin{bmatrix} f(NB_1) \\ f(NB_2) \\ \vdots \\ f(NB_N) \end{bmatrix} \quad (4)$$

**A) The suitability of water collection**

Before evaluating a solution or beetle, the objective function is applied to a randomly generated issue space. More water and moisture may be collected by any beetle whose goal function calculation is larger. Looking at it this way, the beetle in issue is probably situated in an ideal spot, the kind of spot that other beetles will be drawn to in order to find water. Here we may compute the capability of each location to receive many beetles, such as NB, using Equation 5:

$$C_i = C_{max}.sin\left(\frac{f(NB_I) - f_{min}}{f_{max} - f_{min}}.\frac{\pi}{2}\right) \quad (5)$$

$C_i$ is the capacity of the sum of beetles in the area NB, is located. $C_{max}$ is the maximum capacity of the sum of beetles that can be in one area. $f(NB_I)$ shows the beetle population's competence, with NR being the overarching competency and f min and f max being the minimum and maximum competences, respectively. With each iteration, a new set of randomly generated solutions to the problem space can be generated by determining the value of $C_i$. These are fresh ideas, and the beetles who are seeking water can approach whichever of the original insects they like. For two beetles, $f_{min}$ = zero and $f_{max}$ = $C_{max}$, the value of $C_i$ is given below. Using Equation 6, the number of newly formed beetles that will follow the existing insects in collecting water can be determined. A similar extension to Equation 7 is possible for Equation 6. Each beetle's $C_i$, value indicates the degree to which it is noticeable to and attractive to other insects. The entire number of beetles looking for water is represented by C in this relationship:

$$C = \sum_{i=1}^{N} C_i = C_1 + C_2 + \cdots + C_N \quad (6)$$

$$C = \sum_{i=1}^{N} C_{max} sin\left(\frac{f(NB_i)-f_{min}}{f_{max}-f_{min}}.\frac{\pi}{2}\right) = C_{max}.sin\left(\frac{f(NB_i)-f_{min}}{f_{max}-f_{min}}.\frac{\pi}{2}\right) + \cdots + C_{max}.sin\left(\frac{f(NB_i)-f_{min}}{f_{max}-f_{min}}.\frac{\pi}{2}\right) \quad (7)$$

This nonlinear value starts at zero and is increased from there by merit up to C max.

**B) Moving toward wet areas**

It is necessary for any problem solver or beetle to select moist areas to locate water. The moisture surrounding a particular insect can be inferred to act as an attractant, drawing more beetles to that location. The desirability of moisture absorption decreases as the distance from the source increases. Assume that the problem space contains two areas, one inhabited by a beetle-like $NB_i$ and the other by $NB_j$. Using Equation 8, the distance between two beetles $C_i$ and $NB_i$ can be determined, where $C_i$ is a number beetle that plans to approach $NB_i$.

$$d_{ij} = \|NB_i - NB_j\| = \sqrt{\sum_{k=1}^{D}\left(NB_{i,k} - NB_{j,k}\right)^2} \quad (8)$$

It is possible to determine the degree to which a certain location is appealing to beetles using Equation 9. Little bugger $NB_i$ is expected to enter the beetle $NB_j$ is located:

$$Humidity(r) = \rho \times Humidity_0.exp\left(-d_{ij}^m\right) \quad (9)$$

In this regard, $Humidity_0$is the initial humidity level in the problem′s surroundings and space, which might range from 2 to $Humidity(r)$ is the number of areas of the beetle $NB_j$, Here, the power m is considered to be 1.5-2. In this case, $d_{ij}^m$ is the answer to the problem or the distance between the two beetles. The proximity-based coefficient of increase for humidity, as determined by Equation 10, grows with each iteration of the suggested method until it reaches J, at which point it is regarded to be equal to 2. The search shifts from a local to a global one when the repetition level rises because the beetle experiences more wetness as it gets closer to the other insect, leading to an increase in p.:

$$\rho = \rho_{max} - p_0.\left(1 - \frac{iter}{Maxiter}\right).rand(0,1) \quad (10)$$

Specifically, $iter$ is the current repetition sum of the extreme iteration number, coefficient of humidity increase. This coefficient is also the value that beetles feel when they are near more humid areas.

The diagram illustrates that beetles in the final iteration are more sensitive to moisture, either due to their proximity to the ideal solution or their presence in regions with higher moisture absorption coefficients. Equation 11 describes how an insect updates its position based on its current location and the moisture sensing coefficient.

$$NB_j^{new} = NB_j^{old} + Humidity\left(Nb_i - NB_j^{old}\right) + levy \quad (11)$$

In this Equation 11, the current beetle that intends to move are $NB_j^{old}$ and $NB_j^{new}$, correspondingly. The position of a attracts other beetles is designated by $Nb_i$.

Formulated from Equation 1), the levy is an accidental vector for the undertaking of beetles.

$$lev\ y = \frac{u}{|v|^{\frac{1}{\beta}}}.\left|\frac{\Gamma(1+\beta).sin\left(\frac{\pi}{2}\beta\right)}{\Gamma\left(\frac{1+\beta}{2}\right).\beta.2^{\frac{\beta-1}{2}}}\right| \quad (12)$$

u besides v are two single accidental vectors that alteration in the intermission (0, 1) besides B is a constant worth equal to 1.5.

**C) Move the wet mass**

A beetle's keen sense of smell allows them to locate places with more humidity. Modelling this behavior requires knowledge of the beetles' center of gravity as well as the moist places that are used. As in Equation 13, the beetles also look for the area between the ideal solution and the point of gravity. In this case, it is taken for granted that every beetle possesses a certain quantity of water and moisture that may be utilized by locating these fluids' centres of gravity for a more efficient search. Here, the optimum and gravity-rich regions may hold the key to locating water.:

$$NB_i^{new} = N_i^{old} + rand.(NB^+ - \overline{NB}) + levy \quad (13)$$

NB* is the spot with the highest humidity, and NB is the spot where the beetles' bodies are in relation to the water gravity in their surroundings. As shown in Equation 14, NB represents the population gravity point value. The role of $\overline{NB}$ can be reduced to further influence the outcome of Equation 13, allowing for more suitable solutions to be identified as described in Equation 15.

$$\overline{NB} = \frac{\sum_{i=1}^{N} NB_i}{N} = \frac{NB_1 + NB_2 + \cdots + NB_N}{N} \quad (14)$$

$$NB_i^{new} = NB_i^{old} + rand.(p.NB^* - (1-p)\overline{NB}) + levy \quad (15)$$

**D) Hunting or removal of the population**

After being placed on top of a hill and allowed to soak in moisture from the air, beetles make an effort to make their way back to the nest. During this process, lizards prey on some of the beetles. These strategies could become obsolete if a new method for eliminating beetles is introduced. According to the suggested strategy, the likelihood of capturing a beetle or selecting a solution increase as its suitability decreases. This strategy gradually eliminates unsuitable solutions from the population. In this technique, unsuitable solutions can be eliminated using the roulette wheel mechanism, which probabilistically selects candidates for removal based on their suitability. The technique has a high rate of eliminating errors while the problem space generates numerous random solutions through iteration and repetition.

Class imbalance in the ECG dataset was addressed using several techniques. Class weighting was applied to assign higher importance to minority classes, and data augmentation techniques (e.g., time shifting, signal scaling) were used to generate additional samples for underrepresented classes. Additionally, the synthetic minority over-sampling technique (SMOTE) was used to synthetically oversample minority classes, and under-sampling was applied to reduce the dominance of majority classes. The model was evaluated using balanced metrics like the F1-score and area under the precision-recall curve (AUC-PR), which better reflect performance on imbalanced data compared to accuracy.

## 3.4Classification

The suggested model comprises three primary components: a feature extractor, a classifier, and a domain discriminator. Before training the model, the source and target ECG signals were extracted. Spatial information was then captured using a sub-band filter in conjunction with a convolutional layer and CBAM.  Next, temporal data was extracted using a variance layer [37–39]. The next step involves extracting features from the source (Ds) and target (Dt) domains. The data distributions of the two domains were aligned, and domain-invariant feature representations were trained simultaneously, reducing the data distribution discrepancy. This approach improves classification performance on the target domain by leveraging labeled data from multiple individuals in the source domain.

**Feature extractor**

The feature extractor incorporates a module for extracting spatial features and a variance layer for extracting temporal data. These modules work together to improve the efficiency of feature extraction from raw ECG signals, which are connected to tasks [40].

If all the channels in the spatial convolutional module were treated equally, the channels with a stronger joining to motor were given advanced weights. This could lead to poor classification performance because features would be compromised. This is because different motor imagery (MI) tasks stimulate different functional regions of the brains [41–44]. CBAM [45, 46], an efficient module, was incorporated to draw inspiration from attention mechanisms that have been successfully applied in computer vision. By assigning greater weight to channels related to MI and less weight to unrelated channels, the discrimination of the extracted spatial features can be improved [47, 48].

Two modules make up CBAM's attention mechanism: one for channels and one for spaces. With an emphasis on the input's inter-channel interaction, the channel attention unit conducts maxpooling and average-pooling operations. The input is $f \in R^{1\times C\times T}$ , the output is a map $M_c(f)$. The calculation is shown in Equation 16:

$$M_c(f) = \sigma\big(MLP(AvgPool(f)) + MLP(MaxPool(f))\big)$$
$$= \sigma\left(W_1\left(W_0\big(f_{avg}^c\big) + W_1\big(W_0(f_{max}^c)\big)\right)\right) \tag{16}$$

where σ MLP with a solitary hidden layer. $W0, W1 \in R^{1\times 1}$ are weights for inputs. $f_{avg}^c$ and $f_{max}^c$ denote average-pooled max-pooled features respectively. Working in tandem with the channel attention unit, the spatial attention module zeroes in on where relevant components are located. This module can be helpful in ECG-based detection for identifying the specific brain areas that were engaged during MI exercises. This module creates a spatial attention map merging the pooled results. The following is the computation: $M_s(f) \in R^{C\times T}$ . The computation is given as shadows as per Equation 17:

$$M_s(f) = \sigma\big(f^{n\times n}([AvgPool(f); MaxPool(f)])\big)$$
$$= \sigma\left(f^{n\times n}\big(\big[f_{avg}^s; f_{max}^s\big]\big)\right) \tag{17}$$

where σ characterizes the sigmoid function, $f^{n\times n}$ characterizes the filter size n × n. $f_{avg}^s$ and $f_{max}^s$ denote average-pooled correspondingly. In this work, n = 1, while keeping the input signal's original size,

which preserves spatial and temporal info for further extraction, and which can help simplify the model by reducing computing requirements.
Separate, non-overlapping sub-bands were applied to the ECG signals following the attention mechanism. This approach attempted to localize the discriminative info of cardiac-ECG signals, as the mainstream of cardiac-related data lies in the mu ($8-12\,Hz$) and beta (12-32 Hz) bands. The testing findings showed that the 8-30 Hz frequency range outperformed the 4-40 Hz frequency band in terms of categorization ability. Hence, the 8-30 Hz range was chosen for this study. The 4 Hz bandwidth was used to split the frequency band into six sub-bands, ranging from $8-12\,Hz, 12-16\,Hz,..,28-32\,Hz$, where m was the sum of non-overlapping bands. Afterwards, spatial information was extracted using a depth wise convolutional layer. The kernel size was set at (C,1), where C was the sum of electrodes and d was the depth parameter that controlled the number of bands. Therefore, it is possible to combine the spatial data from all of the electrodes into a single electrode.

Using a variance layer, we were able to extract time-related data. It calculates the variance v, which is written as: to get the time series features:

$$v = Var\big(s(t)\big) = \frac{1}{L}\sum_{t=0}^{L-1}(s(t)-\mu)^2 \qquad (18)$$

the input signal s(t), the total sum of period samplings denoted as L, and the mean of s(t) represented by Equation 18.

With the size of the nonoverlapping temporal window fixed as w in this approach, the calculation can be described as follows: the output of the spatial unit was sent to the alteration layer.

$$x_V(k) = \frac{1}{w}\sum_{t=w*k}^{(k+1)*w-1}(x(t)-\mu(k))^2 \qquad (19)$$

w, within the $k^{th}$ window, μ(k) represents the temporal mean of x(t) as per Equation 19.

Due to its importance in influencing the extracted temporal characteristics, the next experimental section will address the effect of window size on classification performance. An excessively large or small size will ultimately impair the findings. The suggested feature extractor's settings are exposed in *Table 1*.

**Table 1** Limits of the projected feature extractor

| Module | Layer | Parameters | Output |
|---|---|---|---|
| Input | - | - | $1\times C\times T$ |
| **Module** | **Layer** | **Parameters** | **Output** |
| | CBAM | 1X1 | $1\times C\times T$ |
| | Sub-band Filtering | m | $m\times C\times T$ |
| | Depth wise Conv2D | $C\times 1, d$ | $d\times m\times 1 \times T$ |
| | Variance Layer | 1XW | $d\times m\times 1 \times T/w$ |
| | FC | 64 | - |

**Domain discriminator**
A domain discriminator and feature extraction are components of the adversarial training method, as stated by Wasserstein generative adversarial network (WGAN). During both the source and target domains. This made it difficult for the domain to determine which domain the feature originated from. In turn, the discriminator attempted to determine the data's domain of origin by measuring the Wasserstein among the distributions of the two domains. Last but not least, the domain discriminator can be fooled by the learnt feature representations, resulting in a minimized Wasserstein distance among the two domains or a reduction in discrepancy. This allowed us to use what we learned in the source domain to improve our data classification in domain by aligning the marginal data domains.

For the discriminator limit $\theta_d$: the appearance for the gradient norm is:$\mathcal{L}_{wd}$ with admiration to limit $\theta_d$:

$$\mathcal{L}_{wd}(x^s,x^t) = \frac{1}{n^s}\sum_{x^s\in} f_w\left(f_g(x^s)\right) - \frac{1}{n^t}\sum_{x^t\in D^t} f_w(f_g(x^t)) \qquad (20)$$

where $x^s$ and $x^t$ are the data tasters' field besides target domain, correspondingly. $f_g$ is a by the map's trials to a illustration with the corresponding parameter $\theta_f$. $f_w$ domain discriminator learns a function that maps feature illustrations to real sums with limits $\theta_d$:.

Capacity underutilization, gradient vanishing or exploding, and other issues that degrade domain adaptation performance might arise if the Lipschitz distance is not satisfied. $\mathcal{L}_{grad}$ the expression is: on the gradient norm for parameter in Equation 21:

$$\mathcal{L}_{grad}(\tilde{h}) = \left(\left\|\nabla_{\tilde{h}} f_w(\tilde{h})\right\|_2 - 1\right)^2 \qquad (21)$$

The source domain and target field are used to extract feature representations, denoted as $\tilde{h}$.

The domain was trained to optimal performance by first optimizing the Wasserstein distance between target domains, as this measure offers superior differentiation and continuity. Next, the parameter $\theta_f$ was used to train the feature extractor, and the fixed simultaneously with the goal of minimizing the Wasserstein distance. This entire procedure is described in the Equation 22 in the following way:

$$\min_{\theta_f} \max_{\theta_d} \{\mathcal{L}_{wd} - \lambda \mathcal{L}_{grad}\} \quad (22)$$

when optimizing the minimal operation to eliminate the impact of the illustration learning procedure, the balance coefficient, denoted as λ, is equal to 0. At long last, adversarial learning allows us to learn domain invariant representations and the Wasserstein zero.

**Classifier**

Thirdly, the feature extractor trains a classifier to anticipate which representations are to be labeled. A SoftMax function and two fully connected layers make it possible to convert the network's predictions into labels for classes. No target feature labels were utilized to train the classifier in this study. Classifier training instead relied solely on source domain labelled cardiac ECG data. The trained classifier was subsequently used for predicting data in the target domain. An approach known as a cross-entropy loss, computed as per Equation 23.

$$\mathcal{L}_{cls} = -E_{x\sim D} \sum_{k=1}^{cls} I_{(y==k)} \log(\mathcal{M}(x)) \quad (23)$$

in where M stands for the suggested model and I is the pointer function that returns 1 when y=k and 0 otherwise.

The following is the final expression for the objective function is shown in Equation 24:

$$\min_{\theta_f, \theta_c} \left\{ \mathcal{L}_{cls} + \mu \max_{\theta_d} \left[ \mathcal{L}_{wd} - \lambda \mathcal{L}_{grad} \right] \right\} \quad (24)$$

where $\theta_c$ is the SoftMax prediction parameter. The parameter ε is responsible for upholding the equilibrium between feature transferability and discrimination. When optimizing the minimum operation, λ equals zero. Here, the parameters are fine-tuned by NBOA, which is described in the section 3.3.2.

# 4.Results

The experiments were showed on a computer with the following specifications: 32 GB of RAM, an NVIDIA Quadro RTX 4000 visual card, and an Intel(R) Xeon(R) W-2245 processor with a CPU@ 3.90GHz 3.91.

## 4.1Analysis of Various models on different classes

*Figure 1* presents the classification accuracy of various ECG classes using different techniques. The gradient convolutional attention block with stacked residual blocks (GCAB-SRB) [16] method achieved accuracies of 95.30% for AFIB, 94.63% for GSVT, 94.87% for SB, and 96.56% for SR. The ResNet [17] model attained 89.51% for AFIB, 90.68% for GSVT, 89.46% for SB, and 90.07% for SR. The 1D-CNN [18] method recorded 93.00% for AFIB, 92.00% for GSVT, 94.00% for SB, and 93.00% for SR. The super-resolution convolutional neural network (SRCNN) [19] technique achieved 94.29% for AFIB, 93.75% for GSVT, 95.74% for SB, and 96.44% for SR. The CSSA-DCNN [20] method reported 95.76% for AFIB, 96.67% for GSVT, 96.99% for SB, and 96.85% for SR. The ECGTransForm [21] approach achieved 94.17% for AFIB, 94.28% for GSVT, 93.76% for SB, and 93.93% for SR. The proposed model outperformed all existing methods, achieving 97.81% for AFIB, 98.31% for GSVT, 97.89% for SB, and 98.10% for SR.

## 4.2Comparative investigation of various deep learning

*Figures 2* and *3* present the experimental analysis of various DL models using an 80%-20% training-to-testing data split. The GCAB-SRB [16] model achieved an accuracy of 93.39%, precision of 93.52%, recall of 93.15%, F1-score of 93.49%, and an AUC of 99.14%. The ResNet [17] model obtained an accuracy of 95.21%, precision of 95.58%, recall of 95.23%, F1-score of 95.33%, and an AUC of 99.21%. The 1D-CNN [18] model reported an accuracy of 92.68%, precision of 91.99%, recall of 92.55%, F1-score of 92.24%, and an AUC of 98.99%. The SRCNN [19] technique achieved an accuracy of 95.80%, precision of 95.79%, recall of 95.44%, F1-score of 95.85%, and an AUC of 99.43%. The CSSA-DCNN [20] method attained an accuracy of 91.45%, precision of 91.82%, recall of 91.67%, F1-score of 91.70%, and an AUC of 97.51%. The ECGTransForm [21] model achieved an accuracy of 96.01%, precision of 95.21%, recall of 96.19%, F1-score of 96.80%, and an AUC of 99.17%. The proposed model outperformed all baselines, achieving an accuracy of 97.14%, precision of 96.48%, recall of 97.26%, F1-score of 97.84%, and an AUC of 99.80%.

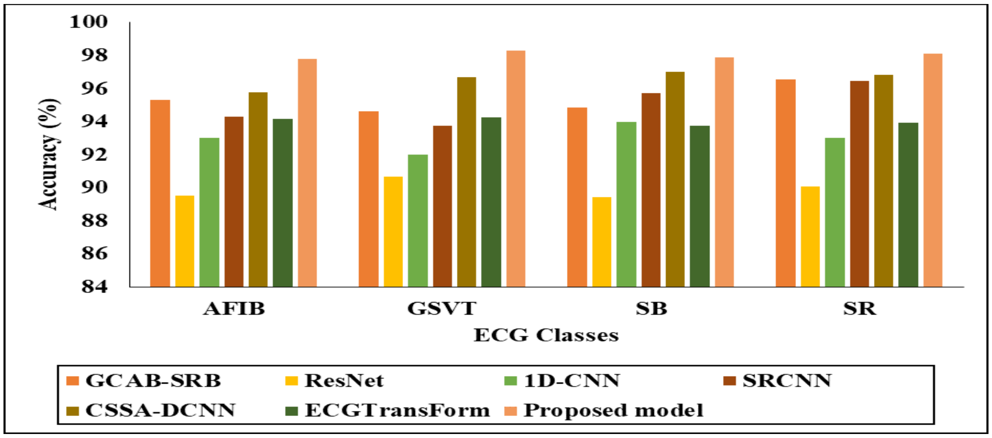


**Figure 1** Graphical analysis of projected model in terms of accuracy

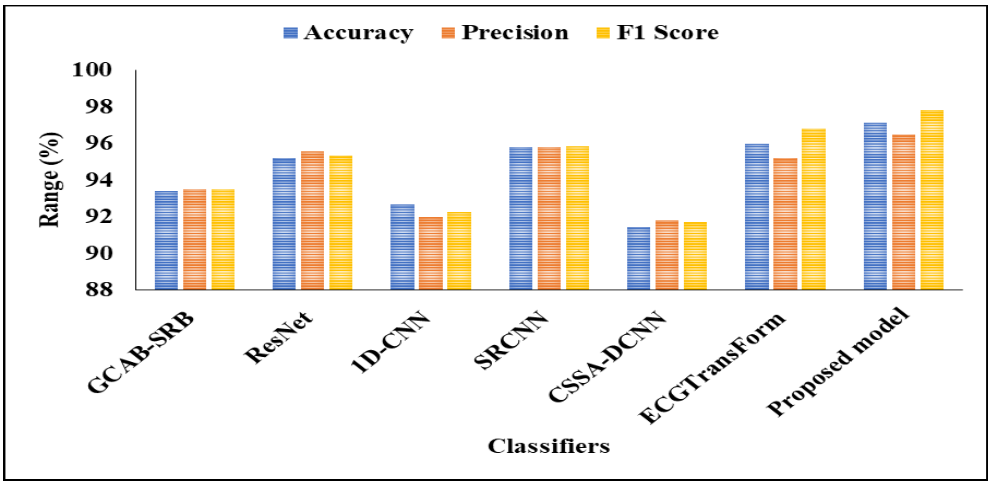


**Figure 2** Visual Illustration of different classifiers

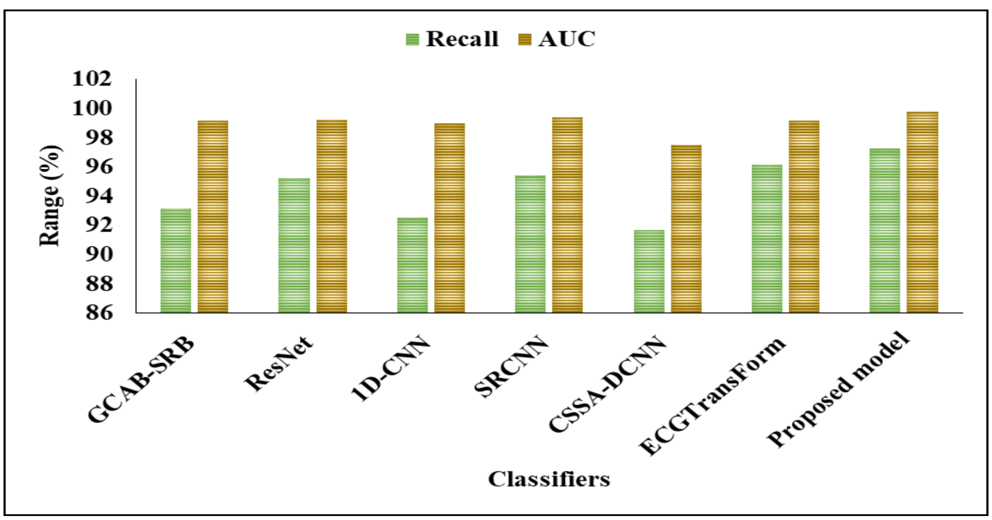


**Figure 3** Graphical description for cardiac arrhythmias classification

# 5.Discussion

## 5.1Key findings and interpretations

In this study, we developed a novel approach for arrhythmia detection using a DAN, incorporating GAM-ResNet18 for feature extraction, attention mechanisms, and the NBOA for optimization. Our model achieved a significant improvement in classification accuracy, especially in detecting underrepresented arrhythmias such as GSVT and SB. Key performance metrics such as accuracy (97.14%), precision (96.48%), and F1-score (97.84%) show that our model consistently outperforms traditional DL models like SRCNN and ECGTransForm, particularly in challenging rhythm classes.

## 5.2Implications of the findings

The high classification performance across various arrhythmia types, particularly in noisy and imbalanced data, indicates that our model has strong potential for real-world clinical applications. The use of domain adaptation and attention mechanisms proved effective in bridging the gap between different patient populations and focusing on key signal features. This reduces reliance on expert interpretation, speeding up diagnosis and improving accuracy in diverse clinical environments. Additionally, the interpretability enhancements make the model more reliable in a sensitive domain like healthcare, where trust and accountability are critical.

## 5.3Comparative analysis

Compared to existing models such as GCAB-SRB, ResNet, and SRCNN, the proposed model demonstrates superior performance across multiple evaluation metrics, particularly in effectively handling imbalanced data. While ResNet models tend to struggle with smaller rhythm classes, our model, with its attention-based approach and domain adaptation, manages to maintain high precision and recall across all classes. *Figure 2* highlights the significant gains in precision (97.26%) and recall (97.84%) for minority classes like GSVT, which are often missed by traditional models. The integration of NBOA further contributed to faster convergence and higher accuracy compared to standard optimizers like Adam.

## 5.4Limitations

Despite these promising results, our study has certain limitations. First, data imbalance remains a challenge. Although techniques such as SMOTE and class weighting were employed, the model exhibited slightly lower recall for extremely underrepresented classes, such as GSVT. Access to larger and more balanced datasets in future studies could enhance performance. Second, interpretability of the model, while improved through the use of attention mechanisms, remains limited. Certain classification decisions—particularly for overlapping arrhythmia types like SVT and AFIB—are still difficult to explain. Advancements in explainable artificial intelligence (XAI) could significantly improve the model's clinical relevance. Third, generalizability is a concern, as the model was evaluated solely on the Chapman dataset. Although the results were strong, broader validation on larger, multi-institutional datasets is necessary to confirm its robustness and applicability across diverse populations.

The results of this study provide strong evidence that the proposed DAN with GAM-ResNet18, attention mechanisms, and NBOA optimization represents a significant advancement in the field of automated ECG analysis. By improving both accuracy and interpretability, this model has the potential to be integrated into clinical workflows, reducing the time and expertise required for arrhythmia diagnosis. Moreover, the ability to maintain high performance on imbalanced data makes it particularly useful for detecting rare arrhythmias, which are often overlooked by traditional methods.

A complete list of abbreviations is listed in *Appendix I.*

# 6.Conclusion and future work

In this study, arrhythmias were classified using attention-based DL algorithms. A GAM-ResNet18 network model was proposed to extract features from ECG data for two-dimensional image recognition. To enhance recognition performance, the GAM global attention mechanism was incorporated into each residual block of the network. Additionally, transfer learning was employed to expedite model training, and the NBOA model was used for parameter optimization during feature extraction. Furthermore, the study introduces a DAN architecture enhanced with Wasserstein distance to improve ECG-based cardiac arrhythmia classification. To address the challenge of limited ECG data, the proposed framework reduces cross-subject variability and improves feature discrimination. Feature extraction was further enhanced by integrating CBAM with adversarial training, contributing to improved classification accuracy.

The results demonstrated that the proposed framework significantly improves the accuracy of cardiac arrhythmia classification. However, despite its strong performance, several limitations must be considered. The dataset used for training and testing had a highly imbalanced class distribution, which may affect the model's generalizability, even after applying class weight adjustments. Moreover, individual variability in cardiac arrhythmias presents an additional challenge.

While the proposed model shows promising outcomes, there is scope for further improvement. Future research could explore architectural refinements, hyperparameter optimization, and the integration of additional clinical features to enhance classification performance. Moreover, prospective validation studies in real-world clinical environments are essential to evaluate the model's practical utility and its potential impact on patient care.

## Acknowledgment
None.

## Conflicts of interest
The authors have no conflicts of interest to declare.

## Data availability
The Chapman-Shaoxing 12-lead ECG dataset used in this study is publicly available on Kaggle at https://www.kaggle.com/datasets/erarayamorenzomuten/chapmanshaoxing-12lead-ecg-database

## Author's contribution statement
**Lakshmi Naga Jayaprada Gavarraju**: Conceptualization, data curation, methodology. **Sandhya K**: Formal analysis, resources, writing-original draft. **Tejesh Reddy Singasani:** Methodology, writing-original draft. **Dileep Pulugu:** Data curation, writing – review and editing. **Lokesh Sai Kiran Vatsavai**: Writing – review and editing. **Usha Rani Bajjuri**: Validation. **Ramesh Vatambeti**: Writing – review and editing.

## References
[1] Ansari Y, Mourad O, Qaraqe K, Serpedin E. Deep learning for ECG arrhythmia detection and classification: an overview of progress for period 2017–2023. Frontiers in Physiology. 2023; 14:1-20.
[2] Daydulo YD, Thamineni BL, Dawud AA. Cardiac arrhythmia detection using deep learning approach and time frequency representation of ECG signals. BMC Medical Informatics and Decision Making. 2023; 23(1):1-14.
[3] Ebrahimi Z, Loni M, Daneshtalab M, Gharehbaghi A. A review on deep learning methods for ECG arrhythmia classification. Expert Systems with Applications: X. 2020; 7:100033.
[4] Kolhar M, Al Rajeh AM. Deep learning hybrid model ECG classification using AlexNet and parallel dual branch fusion network model. Scientific Reports. 2024; 14(1):26919.
[5] Zhang Y, Yi J, Chen A, Cheng L. Cardiac arrhythmia classification by time–frequency features inputted to the designed convolutional neural networks. Biomedical Signal Processing and Control. 2023; 79:104224.
[6] Ayar M, Isazadeh A, Gharehchopogh FS, Seyedi M. Chaotic-based divide-and-conquer feature selection method and its application in cardiac arrhythmia classification. The Journal of Supercomputing. 2022; 78:5856-82.
[7] David S, Duraipandian K, Chandrasekaran D, Pandey D, Sindhwani N, Pandey BK. Impact of blockchain in healthcare system. In Unleashing the potentials of blockchain technology for healthcare industries 2023 (pp. 37-57). Academic Press.
[8] Liu Z, Chen P. Electrocardiogram data recognition algorithm based on variable scale fusion network model. Journal of Biomedical Engineering. 2022; 39(3):570-8.
[9] Kim YK, Lee M, Song HS, Lee SW. Automatic cardiac arrhythmia classification using residual network combined with long short-term memory. IEEE Transactions on Instrumentation and Measurement. 2022; 71:1-7.
[10] Panganiban EB, Paglinawan AC, Chung WY, Paa GL. ECG diagnostic support system (EDSS): a deep learning neural network based classification system for detecting ECG abnormal rhythms from a low-powered wearable biosensors. Sensing and Bio-Sensing Research. 2021; 31:1-15.
[11] Lee H, Yoon T, Yeo C, Oh H, Ji Y, Sim S, et al. Cardiac arrhythmia classification based on one-dimensional morphological features. Applied Sciences. 2021; 11(20):1-11.
[12] Singh PN, Mahapatra RP. A novel deep learning approach for arrhythmia prediction on ECG classification using recurrent CNN with GWO. International Journal of Information Technology. 2024; 16(1):577-85.
[13] Sumalatha U, Prakasha KK, Prabhu S, Nayak VC. Deep learning applications in ecg analysis and disease detection: an investigation study of recent advances. IEEE Access. 2024: 126258-84.
[14] Xiao Q, Lee K, Mokhtar SA, Ismail I, Pauzi AL, Zhang Q, et al. Deep learning-based ECG arrhythmia classification: a systematic review. Applied Sciences. 2023; 13(8):1-25.
[15] Saber M, Abotaleb M. Arrhythmia modern classification techniques: a review. Journal of Artificial Intelligence and Metaheuristics. 2022; 1:42-53.
[16] Petmezas G, Stefanopoulos L, Kilintzis V, Tzavelis A, Rogers JA, Katsaggelos AK, et al. State-of-the-art deep learning methods on electrocardiogram data: systematic review. JMIR Medical Informatics. 2022; 10(8): e38454.
[17] Ding C, Yao T, Wu C, Ni J. Advances in deep learning for personalized ECG diagnostics: a

systematic review addressing inter-patient variability and generalization constraints. Biosensors and Bioelectronics. 2024: 117073.
[18] Kim HK, Sunwoo MH. An automated cardiac arrhythmia classification network for 45 arrhythmia classes using 12-lead electrocardiogram. IEEE Access. 2024; 12:44527-38.
[19] Anand R, Lakshmi SV, Pandey D, Pandey BK. An enhanced ResNet-50 deep learning model for arrhythmia detection using electrocardiogram biomedical indicators. Evolving Systems. 2024; 15(1):83-97.
[20] Darmawahyuni A, Nurmaini S, Tutuko B, Rachmatullah MN, Firdaus F, Sapitri AI, et al. An improved electrocardiogram arrhythmia classification performance with feature optimization. BMC Medical Informatics and Decision Making. 2024; 24(1):412.
[21] Kaniraja CP, Mishra D. A deep learning framework for electrocardiogram (ECG) super resolution and arrhythmia classification. Research on Biomedical Engineering. 2024; 40(1):199-211.
[22] Soman A, Sarath R. Optimization-enabled deep convolutional neural network with multiple features for cardiac arrhythmia classification using ECG signals. Biomedical Signal Processing and Control. 2024; 92:105964.
[23] El-ghaish H, Eldele E. ECG transform: empowering adaptive ECG arrhythmia classification framework with bidirectional transformer. Biomedical Signal Processing and Control. 2024; 89:105714.
[24] Pasha MY, Sharma N, Verma VK, Choudhary A, Sharma R. Deep learning-based ECG analysis for anomaly detection and classification using DCNN. In international conference on emerging technologies and innovation for sustainability (EmergIN) 2024 (pp. 85-91). IEEE.
[25] Mahajan P, Kaul A. Optimized multi-stage sifting approach for ECG arrhythmia classification with shallow machine learning models. International Journal of Information Technology. 2024; 16(1):53-68.
[26] Gupta A, Banerjee A, Babaria D, Lotlikar K, Raut H. Prediction and classification of cardiac arrhythmia. In sentimental analysis and deep learning: proceedings of ICSADL 2022 (pp. 527-38). Springer Singapore.
[27] Hannun AY, Rajpurkar P, Haghpanahi M, Tison GH, Bourn C, Turakhia MP, et al. Cardiologist-level arrhythmia detection and classification in ambulatory electrocardiograms using a deep neural network. Nature Medicine. 2019; 25(1):65-9.
[28] Zhang D, Yang S, Yuan X, Zhang P. Interpretable deep learning for automatic diagnosis of 12-lead electrocardiogram. Iscience. 2021; 24(4).
[29] Ullah A, Anwar SM, Bilal M, Mehmood RM. Classification of arrhythmia by using deep learning with 2-D ECG spectral image representation. Remote Sensing. 2020; 12(10):1-14.
[30] Jin Y, Li Z, Wang M, Liu J, Tian Y, Liu Y, et al. Cardiologist-level interpretable knowledge-fused deep neural network for automatic arrhythmia diagnosis. Communications Medicine. 2024; 4(1):31.
[31] Narotamo H, Dias M, Santos R, Carreiro AV, Gamboa H, Silveira M. Deep learning for ECG classification: a comparative study of 1D and 2D representations and multimodal fusion approaches. Biomedical Signal Processing and Control. 2024; 93:106141.
[32] Sraitih M, Jabrane Y, Hajjam EHA. An automated system for ECG arrhythmia detection using machine learning techniques. Journal of Clinical Medicine. 2021; 10(22):1-22.
[33] Zheng J, Zhang J, Danioko S, Yao H, Guo H, Rakovski C. A 12-lead electrocardiogram database for arrhythmia research covering more than 10,000 patients. Scientific Data. 2020; 7(1):1-8.
[34] Woo S, Park J, Lee JY, Kweon IS. Cbam: convolutional block attention module. In proceedings of the European conference on computer vision (ECCV) 2018 (pp. 3-19).
[35] Zhang H, Liu C, Tang F, Li M, Zhang D, Xia L, et al. Cardiac arrhythmia classification based on 3D recurrence plot analysis and deep learning. Frontiers in Physiology. 2022; 13:1-13.
[36] Murat F, Yildirim O, Talo M, Demir Y, Tan RS, Ciaccio EJ, et al. Exploring deep features and ECG attributes to detect cardiac rhythm classes. Knowledge-Based Systems. 2021; 232:107473.
[37] Hassan SU, Mohd ZMS, Abdullah TA, Husain K. Classification of cardiac arrhythmia using a convolutional neural network and bi-directional long short-term memory. Digital Health. 2022; 8:1-13.
[38] Li J, Pang SP, Xu F, Ji P, Zhou S, Shu M. Two-dimensional ECG-based cardiac arrhythmia classification using DSE-ResNet. Scientific Reports. 2022; 12(1):1-13.
[39] Zhang Y, Liu S, He Z, Zhang Y, Wang C. A CNN model for cardiac arrhythmias classification based on individual ECG signals. Cardiovascular Engineering and Technology. 2022: 548–57.
[40] Li Y, Qian R, Li K. Inter-patient arrhythmia classification with improved deep residual convolutional neural network. Computer Methods and Programs in Biomedicine. 2022; 214:1-10.
[41] Gulrajani I, Ahmed F, Arjovsky M, Dumoulin V, Courville AC. Improved training of wasserstein gans. Advances in Neural Information Processing Systems. 2017; 30.
[42] He J, Rong J, Sun L, Wang H, Zhang Y. An advanced two-step DNN-based framework for arrhythmia detection. In advances in knowledge discovery and data mining: 24th Pacific-Asia conference, Singapore, proceedings, Part II 2020 (pp. 422-34). Springer International Publishing.
[43] Katsushika S, Kodera S, Nakamoto M, Ninomiya K, Inoue S, Sawano S, et al. The effectiveness of a deep learning model to detect left ventricular systolic dysfunction from electrocardiograms. International Heart Journal. 2021; 62(6):1332-41.
[44] Nejedly P, Ivora A, Smisek R, Viscor I, Koscova Z, Jurak P, et al. Classification of ECG using ensemble

of residual CNNs with attention mechanism. In computing in cardiology 2021 (pp. 1-4). IEEE.
[45] Zubair M, Yoon C. Cost-sensitive learning for anomaly detection in imbalanced ECG data using convolutional neural networks. Sensors. 2022; 22(11):1-15.
[46] Labib MI, Nahid AA. OptRPC: a novel and optimized recurrence plot-based system for ECG beat classification. Biomedical Signal Processing and Control. 2022; 72:103328.
[47] Arjovsky M, Chintala S, Bottou L. Wasserstein generative adversarial networks. In international conference on machine learning 2017 (pp. 214-23). PMLR.
[48] Madan P, Singh V, Singh DP, Diwakar M, Pant B, Kishor A. A hybrid deep learning approach for ECG-based arrhythmia classification. Bioengineering. 2022; 9(4):1-15.

**Dr. Lakshmi Naga Jayaprada Gavarraju** (Member of IETE) is working as an Associate Professor in Department of CSE (AI &ML), MRCET, Hyderabad. She completed her M.Tech from JNTUK. She received her Ph.D. Degree for her work on “Novel Evolutionary Algorithms with New Mutants for Sequence Alignment” from Acharya Nagarjuna University. She has an overall teaching experience of 27 years. Her research interests include Machine Learning, Soft Computing and Bio-informatics.
Email: lakshminagajayaprada.g@mrcet.ac.in

**Sandhya K** earned her M. Tech degree in Software Engineering from Jawaharlal Nehru Technological University Anantapur, Andhra Pradesh, India. She is currently an Assistant Professor at Mohan Babu University. Her research interests encompass Software Testing Methods, Software Requirements Analysis, Agile Software Development, and Machine Learning Techniques
Email: sandhyachurchil@gmail.com

**Tejesh Reddy Singasani** lives in Charlotte, North Carolina, and works at Verizon. He's also a PhD student in IT at the University of the Cumberlands. With a solid background in IT industry, Tejesh enjoys diving into new tech challenges and exploring how AI can change the world. He's all about learning and pushing the boundaries of what's possible in tech.
Email: tsingasani19552@ucumberlands.edu

**Dr. Dileep Pulugu** Currently working as Professor in the Department of Computer Science and Engineering in Malla Reddy College of Engineering and Technology, Hyderabad. He is having more than 21 years of teaching and research experience. He obtained his B.Tech(CSE) and M.Tech(CSE) from JNTU, Hyderabad, Telangana State, India. He obtained his Ph.D in Computer Science and Systems Engineering which is in the area of Artificial Intelligence and Machine Learning from Andhra University, Andhra Pradesh State, India. He has published more than 70 research papers with good impact factors in reputed International, National Journals and International Conferences. To his credit, he is having 20 Patents,15 Books published and 5 Book Chapters in CSE domain.
Email: Dileep.p505@gmail.com

**Lokesh Sai Kiran Vatsavai** received his M.Tech in IT from JNTU Kakinada. He has around 1 year of Teaching Experience. He works as Assistant Professor in the Department of Information Technology, SRKR Engineering College, Bhimavaram, India. He has published 3 papers in refereed journals and conference proceedings. His research interests include Deep Learning, Data Science and Automation.
Email: lokesh3069@srkrec.ac.in

**Usha Rani Bajjuri** is a Senior Assistant Professor with the CSE department, Lakireddy Bali Reddy College of Engineering(A), Mylavaram, Andhra Pradesh, India. She is currently pursuing a PhD degree in the field of Deep Learning at JNTUGV, Vizianagaram, Andhra Pradesh, India. With 8 years of Teaching experience, she published three Articles in international journals and Seven papers in international conferences. Her research interests include Machine Learning, Image Processing and the IoT.
Email: bajjuri.usharani2022@gmail.com

**Dr. Ramesh Vatambeti** received his B.Tech from Sri Venkateswara University, Tirupati in Computer Science and Engineering and M.Tech in IT and PhD in CSE from Sathyabama University, Chennai. He has around 20 years of teaching experience from reputed Engineering Institutions. He works as Professor in the School of Computer Science and Engineering at VIT-AP University, Amaravati, India. He has published more than 70 papers in refereed journals and conference proceedings. He is the reviewer for several refereed International Journals and acted as Session Chair and technical committee member for several International

Conferences held in India and abroad. He has successfully guided 3 Ph.D. scholars. His research interests include Computer Networks, Mobile Ad-Hoc and Sensor Networks and Machine Learning.
Email: v2ramesh634@gmail.com

## Appendix I

| S. No. | Abbreviation | Description |
|---|---|---|
| 1 | AF | Atrial Flutter |
| 2 | AFIB | Atrial Fibrillation |
| 3 | AT | Atrial Tachycardia |
| 4 | AUC-PR | Area Under the Precision-Recall Curve |
| 5 | AVNRT | Atrioventricular Nodal Reentrant Tachycardia |
| 6 | AVRT | Atrioventricular Reentrant Tachycardia |
| 7 | CBAM | Convolutional Block Attention Model |
| 8 | CNN | Convolutional Neural Network |
| 9 | CVD | Cardiovascular Diseases |
| 10 | CSSA | Chameleon-Sparrow Search Algorithm |
| 11 | CT | Computed Tomography |
| 12 | DAN | Domain Adaptation Network |
| 13 | DCNN | Deep Convolutional Neural Networks |
| 14 | ECG | Electrocardiogram |
| 15 | GAM | Global Attention Module |
| 16 | GAN | Generative Adversarial Network |
| 17 | GCAB-SRB | Gradient Convolutional Attention Block with Stacked Residual Blocks |
| 18 | GSVT | Generalized Supraventricular Tachycardia |
| 19 | MI | Motor Imagery |
| 20 | MMD | Maximum Mean Discrepancy |
| 21 | MRI | Magnetic Resonance Imaging |
| 22 | NBOA | Namib Beetle Optimization Algorithm |
| 23 | ResNet | Residual Network |
| 24 | RNN | Recurrent Neural Network |
| 25 | SAAWR | Supraventricular Arrhythmia with Aberrant Waveform Rhythm |
| 26 | SI | Sinus Irregularity |
| 27 | SINT | Sinus Intermittent Rhythm |
| 28 | SB | Sinus Bradycardia |
| 29 | SMOTE | Synthetic Minority Over-sampling Technique |
| 30 | SR | Sinus Rhythm |
| 31 | SRCNN | Super-Resolution Convolutional Neural Network |
| 32 | STFT | Short-Time Fourier Transform |
| 33 | SVT | Supraventricular Tachycardia |
| 34 | VGG | Visual Geometry Group |
| 35 | WGAN | Wasserstein Generative Adversarial Network |
| 36 | XAI | Explainable Artificial Intelligence |